PB90-197831

Diagnostic Studies of Ozone in the Northeastern United States Based on Applications of the Regional Oxidant Model (ROM)

(U.S.) Environmental Protection Agency, Research Triangle Park, NC

May 89

U.S. Department of Commerce
National Technical Information Service
NTIS

TECHNICAL REPORT DATA
(Please read Instructions on the reverse before completing)

1. REPORT NO.	2.	3. RECIPIENT'S ACCESSION NO.
600/D-89/011		PB90 197831/AS

4. TITLE AND SUBTITLE	5. REPORT DATE
DIAGNOSTIC STUDIES OF OZONE IN THE NORTHEASTERN UNITED STATES BASED ON APPLICATIONS OF THE REGIONAL OXIDANT MODEL (ROM)	1989
	6. PERFORMING ORGANIZATION CODE
7. AUTHOR(S)	8. PERFORMING ORGANIZATION REPORT NO.
R.G. Lamb	
9. PERFORMING ORGANIZATION NAME AND ADDRESS	10. PROGRAM ELEMENT NO.
same as 12	A101/B/63/21 - 1335 (FY-88)
	11. CONTRACT/GRANT NO.
12. SPONSORING AGENCY NAME AND ADDRESS	13. TYPE OF REPORT AND PERIOD COVERED
Atmospheric Sciences Research Laboratory -- RTP, NC Office of Research and Development U.S. Environmental Protection Agency Research Triangle Park, NC 27711	Final Proceedings
	14. SPONSORING AGENCY CODE
	EPA/600/09

15. SUPPLEMENTARY NOTES
APCA Specialty Conference on The Scientific and Technical Issues Facing Post-1987 Ozone Control Strategies, Hartford, CT, Nov. 16-19, 1987

16. ABSTRACT

This paper describes the diagnostic study of the ozone problem in the Northeastern United States based on simulations performed with the Regional Oxidant Model (ROM) and numerical evaluation of individual terms in the equations that form the basis of this model. The study delineates where and in what quantity ozone is generated and where and in what quantities ozone and its precursor species are transported. The relative merits of various emissions control plans are assessed by comparing how each alters the magnitudes and spatial patterns of ozone generation and transport.

17. KEY WORDS AND DOCUMENT ANALYSIS

a. DESCRIPTORS	b. IDENTIFIERS/OPEN ENDED TERMS	c. COSATI Field/Group

18. DISTRIBUTION STATEMENT	19. SECURITY CLASS (This Report)	21. NO. OF PAGES
RELEASE TO PUBLIC	UNCLASSIFIED	21
	20. SECURITY CLASS (This page) UNCLASSIFIED	22. PRICE

EPA Form 2220-1 (Rev. 4-77) PREVIOUS EDITION IS OBSOLETE

PB90-197831

EPA/600/D-89/011
May 1989

DIAGNOSTIC STUDIES OF OZONE IN THE NORTHEASTERN UNITED STATES BASED ON APPLICATIONS OF THE REGIONAL OXIDANT MODEL (ROM)

By

Robert G. Lamb *
Atmospheric Sciences Research Laboratory
U.S. Environmental Protection Agency
Research Triangle Park, NC 27711

EPA Project Officer
K. L. Schere

*On assignment from the National Oceanic and Atmospheric Administration

ATMOSPHERIC SCIENCES RESEARCH LABORATORY
OFFICE OF RESEARCH AND DEVELOPMENT
U.S. ENVIRONMENTAL PROTECTION AGENCY
RESEARCH TRIANGLE PARK, NC 27711

REPRODUCED BY
U.S. DEPARTMENT OF COMMERCE
NATIONAL TECHNICAL INFORMATION SERVICE
SPRINGFIELD, VA. 22161

NOTICE

This document has been reviewed in accordance with U.S. Environmental Protection Agency policy and approved for publication. Mention of trade names or commercial products does not constitute endorsement or recommendation for use.

DIAGNOSTIC STUDIES OF OZONE IN THE NORTHEASTERN UNITED STATES BASED ON APPLICATIONS OF THE REGIONAL OXIDANT MODEL (ROM)

Robert G. Lamb*
U.S. Environmental Protection Agency
Atmospheric Sciences Research Laboratory
Research Triangle Park, NC 27711

* On assignment from the National Oceanic and Atmospheric Administration

The equations that form the basis of air pollution models are mathematical descriptions of the physical and chemical processes that control the concentrations of each chemical species in the atmosphere. Since each term in the basic equations represents a separate physical or chemical process that plays a role in pollution phenomena, evaluating each term individually yields a quantitative measure of the relative importance of each process. Information on the relative significance of individual processes can be valuable in diagnosing the cause of air quality problems in specific areas and in designing emissions control plans that can correct specific problems most effectively.

This paper describes the diagnostic study of the ozone problem in the Northeastern United States based on simulations performed with the Regional Oxidant Model (ROM) and numerical evaluation of individual terms in the equations that form the basis of this model. The study delineates where and in what quantity ozone is generated and where and in what quantities ozone and its precursor species are transported. The relative merits of various emissions control plans are assessed by comparing how each alters the magnitudes and spatial patterns of ozone generation and transport.

Introduction

The Regional Oxidant Model (ROM) was developed to assist the formulation of emissions control strategies to attain the National Ambient Air Quality Standard (NAAQS) for ozone. In this role the model is used to predict the concentration changes that would result from specified emission changes. In this paper we use the ROM in an entirely different role: to diagnose the cause of high ozone concentrations and to reveal the physical processes through which given emissions changes bring about concentration changes. We focus on the simulation of a single, high ozone day in 1980 (20 July), decomposing the ozone fields into the contribution made at each site by horizontal and vertical transport and by chemical production and decay. We perform these analyses on the results of three separate simulations. One simulation used what we refer to as base case emissions. The other two simulations were performed using inventories that represent VOC emissions control strategies based on State Implementation Plans (SIPs). Comparing the results of the three experiments reveals useful insights into the nature of the ozone phenomenon and the problem of ozone control.

The results presented here are only preliminary findings. More definitive results will require simulations of many more meteorological scenarios, a refined base case emissions inventory, and completion of the ROM verification study.

We first summarize essential features of the ROM and discuss the manner in which the results of a regional scale air quality model are properly used. We follow these discussions with a brief presentation of comparisons of model predictions and observations. These data are meant to provide at least a partial basis for judging the credibility of the findings we present in this paper.

Basic Features of the Regional Oxidant Model

The ROM is an Eulerian, episodic model that simulates the hourly concentrations of chemical species with a spatial resolution of about 18.5 km over an area of roughly 1200 x 800 km. The model has 3 1/2 layers whose thicknesses vary in space and time to track meteorological phenomena. Meteorological inputs to the model are derived from observational data, supplemented with physical principles (For further details see refs. 1,2).

The ROM incorporates the Carbon Bond-IV chemical mechanism[3] which simulates some 70 reactions among 28 species. A major feature of the Carbon Bond-IV mechanism is explicit treatment of isoprene, one of the principal constituents of hydrocarbons from natural sources.

The base emissions inventory currently employed in the ROM consists of the 1980 NAPAP 5.3[4] data to describe anthropogenic sources, and a biogenic emissons data base prepared within the Atmospheric Sciences Research Laboratory[5]. The latter is based on estimates of the dry foliar mass of 61 species of trees, 10 types of field crops and two groups of grasses compiled for each grid cell from detailed Forest and Agricultural Service records. The biomass data are combined with empirical emissions factors for each species and hourly temperature, sunlight and cloud cover data to yield biogenic hydrocarbon emissions rates that vary hourly depending on local weather conditions in each grid square.

The ROM is essentially a large system of interconnected submodels and data processing modules that are operated and maintained in strict conformance with a set of quality assurance procedures. These involve both machine

and human checks of computer code, the input and output data streams of each submodule, and the behavior of the model overall. The quality assurance procedures impose a large overhead on the model operations, but they help ensure that ROM results reflect scientific knowledge rather than the artifacts of human errors.

Restrictions on the Use of Model Results

An essential prerequisite to model applications is understanding the type of information that the model is capable of providing. This knowledge is important not only for the "decision makers" who rely on the model as an information resource, but also for the model developers faced with the task of establishing performance standards for model evaluation studies. In this regard the output of any model can be classified into one of two categories: deterministic or stochastic. Since it is beyond the scope of this paper to define these terms rigorously, we will describe them using examples. Underlying concepts will also be presented in an informal vein. For a more thorough discussion, see ref. 6.

The output of a model is stochastic if any of the inputs to the model is stochastic or if the solutions of the equations on which the model is based are stochastic. If all inputs and the equation solutions are deterministic, the model output is deterministic. The Gaussian plume model is an example of a model with deterministic output. In this case one could expect the concentration predicted by the model at a specific site to agree with the concentration value measured at that site, assuming of course that the inputs to the model are accurate and meteorological conditions are compatible with the constraints under which the Gaussian model applies. The extensive role that the Gaussian model has played in air quality engineering is perhaps largely responsible for the general notion that the predictions of any air quality model should agree with measurements made at the location and time corresponding to the prediction. This notion is in principle correct in the case of models with deterministic output, but not in cases where the output is stochastic.

Examples of stochastic models, applicable to dispersion problems of the same type addressed by the Gaussian model, are the so-called large eddy simulation (LES) models of the planetary boundary layer. The inputs to these models are deterministic but the solutions of the model equations are stochastic. If one were to compare the predictions of one of these models, which generally have time resolutions of the order of several seconds, with measurements, one would generally find zero correlation between the predicted and observed values over both space and time. However, if one were to compute statistical properties of the model output -- such as frequencies of occurrence of values, means, variances and the like -- and compare these with corresponding statistics of the measured data one would find good agreement for certain statistics. The point here is that in the case of stochastic models, it is the statistical properties of the individual values given by the model that contain significant information and not the individual output values themselves.

The ROM is another model of the stochastic type. Its governing equations have deterministic solutions, but some of the inputs to the model, particularly the wind fields, are stochastic. Consequently, the ROM should be looked upon as a means of predicting concentration frequencies, spatial patterns in mean values and frequencies, and similar statistical information rather than a means of predicting the concentration that will occur at a specific place at a specific time. This restriction is not inconsistent with the objectives of ozone modeling which, in applications related to the primary standard, is to determine the frequency with which concentrations

will exceed a given level.

Comparison of ROM Predictions with Observations

In accordance with the arguments made in the preceeding section, we offer here as an interim measure of the ROM's performance a comparison of the cumulative frequency distribution of predicted hourly-averaged ozone concentrations in the period 14 July to 26 July 1980 with the corresponding distribution of observed concentrations at 215 U.S. and Canadian surface monitoring stations. The comparisons are given in Figure 1 in the form of quantile-quantile (QQ) plots. In these graphs the ordinate of a point (represented by a + or a digit) is the concentration associated with the specified quantile of the distribution of predicted values while the abscissa is the corresponding concentration in the observations. If the frequency distributions of the predictions and observations were identical, the points of the QQ plot would lie along the straight line shown in each of the graphs. The dashed lines mark the area within which the quantiles of the predicted and observed values agree within ±10%.

For reasons associated with the stochastic nature of the ROM output discussed earlier, the data have been divided into three groups depending in part on the proximity of the measuring station to major NO_x or VOC sources. The group labeled "near source" (the top panel of Figure 1) consist of stations located within or adjacent to ROM grid cells containing major sources. The group labeled "remote" contain stations that are farthest from major sources. The "intermediate" group contains all stations in between these extremes, and it contains the bulk of the data -- 185 of 215 stations.

There are two disparities between the predicted and observed concentration data that will tend to bias the comparisons. One is that the measurements are made at points in space whereas the predictions represent volume averages over grid cells, which are roughly 20 km on a side and 100 meters or so deep. Thus, in areas where there are significant spatial variations in ozone concentration of scales smaller than 20 km, point measurements would tend to scatter on either side of precise predictions. The second disparity is that the predicted values plotted in Figure 1 are from Layer 1 of the model rather than the surface layer, Layer 0, where the measurements are taken. The Layer 0 concentrations are provided by a post-processor of the ROM which is not yet operational. Under stable nighttime conditions the Layer 1 ozone concentrations may be considerably higher than those in Layer 0 due to the effects of deposition. Therefore, to minimize bias we use only data from the daylight hours 0800-1800 in the comparisons.

The relationship between the predicted and observed concentrations evident in Figure 1 follows the general pattern we just outlined: underestimation of peak values and overestimation of minima. This trend is most pronounced at points near major sources, where one would expect the largest small scale spatial fluctuations. At the remote sites, where one would expect the least effect of fluctuations, the frequency distributions of the observed and predicted values agree to within ±10% from roughly the 40-th percentile up to the maximum value, or 100-th percentile. The accentuated overprediction of low concentrations at the remote sites is apparently due to the close proximity of most of these receptors to the lateral boundaries of the ROM. Specifying the inflow boundary concentrations in a model of this scale is fraught with uncertainty. At the intermediate range sites, agreement within ±10% exists from about the 60-th to the 99-th percentiles.

A thorough evaluation of the ROM is now underway using 50 days of simulated ozone, NO_x and hydrocarbon concentrations and observed data from both U.S. and Canadian monitoring sites, and a 1980 field study in the Northeast U.S. A major problem faced by the model evaluation effort is that it is virtually impossible to test the performance of the model in the role in which it will be applied, namely estimating the concentration changes that will result from specified emissions changes. The prevailing philosophy is that the ability to predict absolute concentration levels well is a necessary condition for predicting concentration changes accurately. We hope that our evaluation study will have resolved the model performance issues before the ROM is used in studies that will influence emissions control policies. Our use of the model in the present paper is simply to uncover the basic physical processes responsible for the ozone phenomenon. We see nothing in Figure 1 or in any of the other ROM performance data that we have collected to date that would cast doubts on the credibility of the results we are about to describe.

The Roles of Transport and Chemical Production in Regional Ozone

In the remainder of this paper we describe preliminary findings from a study that uses the ROM to diagnose the causes of high ozone in the Northeastern U.S. and the effectiveness of VOC emissions controls. Although the present study focuses on a single day from a 15-day simulation, we expect that once we have completed the analysis of the entire period the results will substantiate the basic findings reported here.

We consider 20 July 1980 which lies midway in the 15-day simulation from which the data given in Figure 1 were taken. On this day a cold front moved into the northwest corner of the model domain during the early morning and stalled by midday along a line running along the Great Lakes into northern New York and on into northern Maine. Cloudiness, showers and thunderstorms occurred along the front throughout the day, while to the south of the front the weather was generally partly cloudy with afternoon temperatures in the mid 90's and dew point temperatures in the 70's. Surface winds were generally southerly to southwesterly over the entire model area during the day.

Figure 2 shows the distribution of the maximum hourly ozone predicted by the model for this day. The overall pattern of the peak concentrations is supported by the monitoring data, some of which are indicated by numbers in the figure.

Current studies of the ozone nonattainment problem are concerned partly with the role of transport. To assist these investigations we have developed a post-processor for the ROM that breaks down the predicted concentrations of each of the 28 simulated species into the separate contributions made by transport, chemical processes and emissions. We can illustrate the process for the case of ozone with the aid of Equation 1, which is a condensed form of the differential equation used in the ROM to simulate ozone:

$$\frac{\partial O_3}{\partial t} = \underbrace{\left(u\frac{\partial O_3}{\partial x} + v\frac{\partial O_3}{\partial y}\right)}_{H} + \underbrace{F_{O_3}}_{V} + \underbrace{k_2(O)}_{P} - \underbrace{O_3[k_3(NO) + k_7(NO_2) + \ldots k_{65}(ISOP)]}_{D} \qquad (1)$$

Here O_3, NO, O etc. denote the concentrations of ozone, nitric oxide, atomic oxygen, and so on. The terms u and v represent the horizontal components of the wind velocity and the k's are chemical rate constants, some of which are functions of sunlight and cloud cover in addition to temperature and air density. The labels H, V, P and D written beneath each term in the equation refer, respectively, to horizontal transport; vertical flux, including deposition; chemical production; and chemical decay. The equations for primary species such as NO also contain an emissions term, E. The post-processor performs a post facto evaluation of each of the five terms for any species, grid cell and time step of interest.

Figure 3 shows the 24-hour averaged total transport, (H+V), of ozone simulated for 20 July. Only the shaded areas in the figure had net import of ozone on this day. Comparing these results with Figure 2 we find that practically all of the areas where the peak simulated concentration exceeded 100 ppb were exporters of ozone. According to the model only portions of the Appalachians farthest from major sources together with the major NO_x source areas themselves had a net import of ozone on this day. This result is at odds with the perception that nonattainment in portions of the Northeast is due in part to the import of ozone from outside sources. According to the model, on this particular day all parts of the Northeast were net sources of ozone with the exception of the major NO_x source areas (which were shown in Figure 3 to be net importers of O_3). These areas are ozone sinks (and NO_2 sources).

The strongest O_3 source areas can be seen in Figure 4 in the isopleths of daily averaged net O_3 production, (P-D). The generation rate over Connecticut ranges from about 50 to 100 ppb/day. Over parts of New Jersey it exceeds 150 ppb/day.

The temporal relationship between transport and production is shown in Figure 5 for the rural Connecticut site marked in Figure 4. Keep in mind that the hourly ozone, net production, and transport values plotted in Figure 5 are from Layer 1 of the ROM and not from the ground-level layer, Layer 0. The simulated diurnal variations indicate that during the predawn hours transport into the receptor cell fluctuated between small positive and negative values while net production of ozone remained slightly negative. The ozone concentration during this time was nearly steady at about 80 ppb. Following sunrise, net production climbed rapidly to a level near 8 ppb/hr which it maintained until about 1100. During this period transport began a negative trend (ozone export) which intensified until noon. The ozone concentration reached a maximum value at about 1100 when the export rate first equaled the rate of production. From that time until shortly after sunset, export exceeded production and as a result the ozone concentration declined steadily. In the early evening there was an influx of ozone from some outside source which led to a secondary ozone maximum. In summary, the peak ozone concentration at this rural site on this day was caused by ozone generated locally. The import of ozone increased concentrations briefly during the evening hours, but over a 24-hour period this site exported considerably more ozone than it imported.

One might wonder why only the small area shown in Figure 3 has a net import of ozone when the generation of this species is so widespread. The answer is that during the day when generation is in progress, the decay rate of ozone is also high as a result of its reactions with NO, NO_2, hydrocarbons and other species. Using the local ozone concentration and the decay rate D, we can compute a local mean life time for ozone molecules. Figure 6 shows the distribution of the average lifetime during the daylight

hours 0600-1800 of the day of the simulation. Note that in the areas of maximum ozone generation, the mean lifetime of ozone was less than 2 hours. This means that in these areas with a 10 mph wind, over 65% of ozone molecules were destroyed within 20 miles of the point of their generation. Figure 6 shows that the lifetime of ozone increases with distance from major sources; and it was an order of magnitude larger nearly everywhere at night.

Let us now look at how a particular VOC emissions reduction strategy alters ozone and its net production rate. We consider first the projected 1987 baseline emissions based in the 1980 base inventory, taking into account both growth and VOC reductions from New Source Performance Standards controls. Both the NO_x and natural hydrocarbon emissions are the same in the projected emissions as in the 1980 base inventory. In general the projected 1987 VOC emissions are 8% lower in attainment counties. In nonattainment areas they are lower by 4% to 48% lower depending on the county. Figure 7 shows where the largest absolute reductions occur. Only areas with VOC reductions of more than 1000 kg/hr (per ROM grid cell) are shown.

We emphasize that the simulations of both the base and projected 1987 emissions, span a 15 day period that begins 8 days before the day we are using here as an example (20 July). Consequently, in the controlled emissions case conditions at the start of 20 July have been altered by the emissions changes. Let us look now at the simulated effects of the VOC emissions reductions.

Figure 8 shows the average net production (P-D) of ozone in the base case on 20 July minus the corresponding value in the controlled case. That is, Figure 8 shows the effect of the emission changes on the effective base case ozone source strength plotted in Figure 4. Comparing Figures 7 and 8 we see that the largest reduction in the ozone production rate occur at the sites of the largest reduction in VOC. Production rates are reduced by 10 to 60 ppb/day in a fairly narrow region around Detroit and the Washington-New York City Corridor, but there is virtually no change in the broad area of high production shown in Figure 4 that stretches across Pennsylvania into Eastern Ohio. A particularly notable change is the increase in the ozone production rate in predominantly rural areas downwind of the Corridor. One of these areas includes the site we examined earlier in Figure 5, and we will return to it shortly.

The change in the maximum hourly ozone concentrations effected by the VOC reductions is shown in Figure 9. On this day the peak concentration is reduced by less than 4 ppb everywhere except areas around Detroit and the Eastern Corridor where reductions up to 29 ppb occur. Comparing Figure 9 with Figure 8 we see that the areas of concentration change have plume-like patterns extending downwind of the locations of change in the ozone source strength. Note that concentrations are not higher around the areas where the ozone production rate was increased by the VOC emissions reductions. The reason can be seen in Figure 10 which compares the hourly ozone and net production rates in the base and control cases at the rural Connecticut site that we examined earlier. We note that with the reduced emissions the ozone concentration drops much more rapidly during the predawn hours than it does in the base case. The model output shows that this is due to the import of lower upwind O_3 concentrations. However, after sunrise the ozone concentration rises much more rapidly in the controlled case because, as we see in the plots of net production, ozone is generated more rapidly. The vertical flux profile V (not shown) shows a fumigation of material into Layer 1 beginning at the same time that the net production rate first exceeds the base case level. It is not

until after transport has increased enough to export ozone faster than it is being generated that the controlled case ozone production rate drops back to the base case level. Were it not for the higher production rate, the peak ozone concentration at this site in the controlled case would be about 30 ppb lower than the base case peak rather than only 10 ppb lower. Further analyses of the precursor species behavior will be necessary before we can explain the higher production rate.

Finally, we present in Figure 11 a comparison of the cumulative frequency distribution of hourly ozone concentrations in the base and controlled cases over 14 days of the simulation. The results are given in the form of the quantile-quantile plots used earlier, with the results grouped according to whether they are within or outside Metropolitan Statistical Areas (MSAs). The points marked CNTRL 1 in the Figure represent the projected 1987 baseline emissions that we have been discussing. The points marked CNTRL 2 are from a second emissions control simulation in which the VOC reductions assumed in CNTRL 1 are increased further to reflect Federal Motor Vehicle Control Program projections to 1995. Overall, in attainment counties VOC emissions are 30% lower than the base case level in CNTRL 2; 8% lower in CNTRL 1. In nonattainment counties, VOC emissions reductions vary from county to county according to the SIPs in CNTRL 1; and in CNTRL 2 the reductions are 22% of the base below the CNTRL 1 levels.

Figure 11 shows that the effects of the controls are nearly the same over the MSA and non-MSA sites, and that the largest reductions in ozone concentration occur where the concentrations are highest. There is practically no change in concentrations below roughly the 95-percentile level. This is a result largely of the design of the control strategy, which imposes the largest emissions reductions on the source areas that affect concentrations in the areas where the highest levels are observed. Note that the maximum concentration reached in CNTRL 2 is about 15 ppb lower than the peak in CNTRL 1. We estimate that a reduction of about 60 ppb below the CNTRL 1 peak level would be necessary to achieve the primary standard, taking into account the ROM's underprediction of peak concentrations.

Conclusions

Following is a summary of the major preliminary findings of the model studies reported here:

(1) In all areas where the maximum daily ozone concentration exceeds 120 ppb, the ozone is generated anew each day from imported and locally emitted precursor species. Over the course of a day these sites export more ozone than they import. Net daily import of ozone occurs only in areas remote (> 100 km) from major NO_x/VOC source areas and within major NO_x source complexes.

(2) During daylight hours when ozone is being generated the average lifetime of an ozone molecule is (roughly) less than 2 hrs within about 50 km of major sources, 2 to 4 hours between 50 and 100 km of major sources, and 4 to 12 hours at greater distances. The lifetimes of ozone during darkness is generally an order of magnitude larger than the daylight values. This means that the peak O_3 concentrations seen during the day in urban areas are not transported overnight into rural areas.

(3) VOC emissions reduction projected for 1987 reduce the rate of generation of ozone in urban areas but they can cause a slight increase in

the production rate of ozone in adjacent rural reas. As a result the emissions reductions are more effective in lowering urban ozone than they are in lowering rural ozone levels.

(4) In a simulation of a 15-day period in July 1980 VOC emissions reductions projected to 1995 (with no NO_x reductions from 1980 emission levels) reduced peak hourly O_3 concentration in the Northeast by about 45 ppb from 1980 levels. It is estimated that an additional reduction of about 60 ppb would be necessary to achieve the current primary standard.

References

1. R. G. Lamb, "A Regional Scale (1000 km) Model of Photochemical Air Pollution: Part 1. Theoretical Formulation", EPA Report # EPA-600/3/83-035 (1983).

2. R. G. Lamb, "A Regional Scale (1000 km) Model of Photochemical Air Pollution: Part 2. Input Processor Network Design", EPA Report # EPA-600/3-84-085 (1984).

3. G. Z. Whitten and M. W. Gery, "Development of CBM-X Mechanisms for Urban and Regional AQSMs", EPA Report # EPA/600/3-86/012 (1986).

4. D. A. Toothman, J. C. Yates and E. J. Sabo, "Status Report on the Development of the NAPAP Emission Inventory for the 1980 Base Year and Summary of Preliminary Data", EPA Report # EPA-600/7-84-091 (1984).

5. J. H. Novak and J. A. Reagan, "Comparison of Natural and Manmade Hydrocarbon Emissions Inventories Necessary for Regional Acid Deposition and Oxidant Modeling", 79th Annual Meeting of the Air Pollution Control Association, Minneapolis, MN (June 1986).

6. R. G. Lamb, "Air pollution models as descriptors of cause-effect relationships", Atmos. Environ. 18: 591-606 (1984).

Acknowledgments

I am indebted to all the members of the ROM team for his or her essential contribution to the work reported here. These include my colleagues in EPA: Joan Novak, Ken Schere, Jim Reagan, Alfreida Rankins, Russ Bullock and Barbara Hinton; and the support staff of the Computer Sciences Corporation: Maureen Barrett, Terri Birth, Trudy Boehm, Carlie Coats, Adrienne Dion, Jeanne Eichinger, Susan Gerry, Dianne Grimes, Mike Harrell, Don Olerud, Kathy Rea, Shawn Roselle, Chet Wayland and Jeff Young. I am especially grateful to Jeff Young for his tireless efforts in getting the ROM post-processor used in this study constructed and operational in record time, and to Trudy Boehm and Dianne Grimes for their special contributions.

Figure Captions

1. Comparison of cumulative frequency distributions of observed (abscissa) and predicted (ordinate) hourly O_3 during the period 14-26 July 1980. Solid lines represent perfect agreement; dashed lines mark ±10% discrepancy bounds. Digits mark decile points, e.g., "0" = 100 percentile or maximum value; "9" = 90-th percentile; etc. The symbol "+" marks integer quantile points except where indicated otherwise. Top panel represents receptor sites in the immediate vicinity of major sources. The middle panel represents receptors between about 5 and 150 km of major sources; and the bottom panel represents receptors farther than about 150 km of major sources.

2. Maximum hourly averaged ozone concentration predicted for 20 July 1980 using base level emissions.

3. Average O_3 transport (horizontal + vertical) for 20 July 1980. Shaded areas had net import of ozone on this day. All other areas were net exporters. Results for Layer 1 only.

4. Average net production (production - decay) of O_3 for 20 July 1980. Dotted areas are ozone sinks. All other areas are sources. Results for Layer 1 only.

5. Hourly variations of ozone, transport (H+V), and net ozone production (P-D) at the rural Connecticut site marked in Figure 4. Negative transport signifies export of ozone; positive values indicate import. Results for Layer 1 only.

6. Mean lifetime (1/e decay time) of ozone molecules during the daylight hours, 0600-1800 EST, on 20 July 1980. Lifetimes are an order of magnitude larger at night.

7. Reduction in VOC emissions (kg/hr/grid cell) from the 1980 base levels projected to the 1987 baseline emissions. Only areas with more than 1000 kg/hr/cell reductions are shown. This is referred to in the text as control strategy #1 or CNTRL1. The NO_x and natural hydrocarbon emissions in this strategy are unchanged from the base levels.

8. Change in the daily net production of ozone on 20 July 1980 effected by control strategy #1 (see Figure 7). Dotted areas mark sites where the ozone production rate is higher with the controlled emissions than with the base, shown in Figure 4. All other areas have reduced production.

9. Changes in the daily maximum ozone concentration on 20 July 1980 achieved by control strategy #1.

10. Comparison of hourly ozone concentration and net ozone production rate between the base and controlled emissions cases at the rural Connecticut site indicated in Figure 4. The base case concentration and net production profiles shown here are identical to those of Figure 5.

11. Simulated effects of two VOC control strategies on the cumulative frequency distributions of hourly ozone during 13-26 July 1980 at MSA and non-MSA sites. See text for descriptions of the emissions controls in strategies CNTRL1 and CNTRL2.

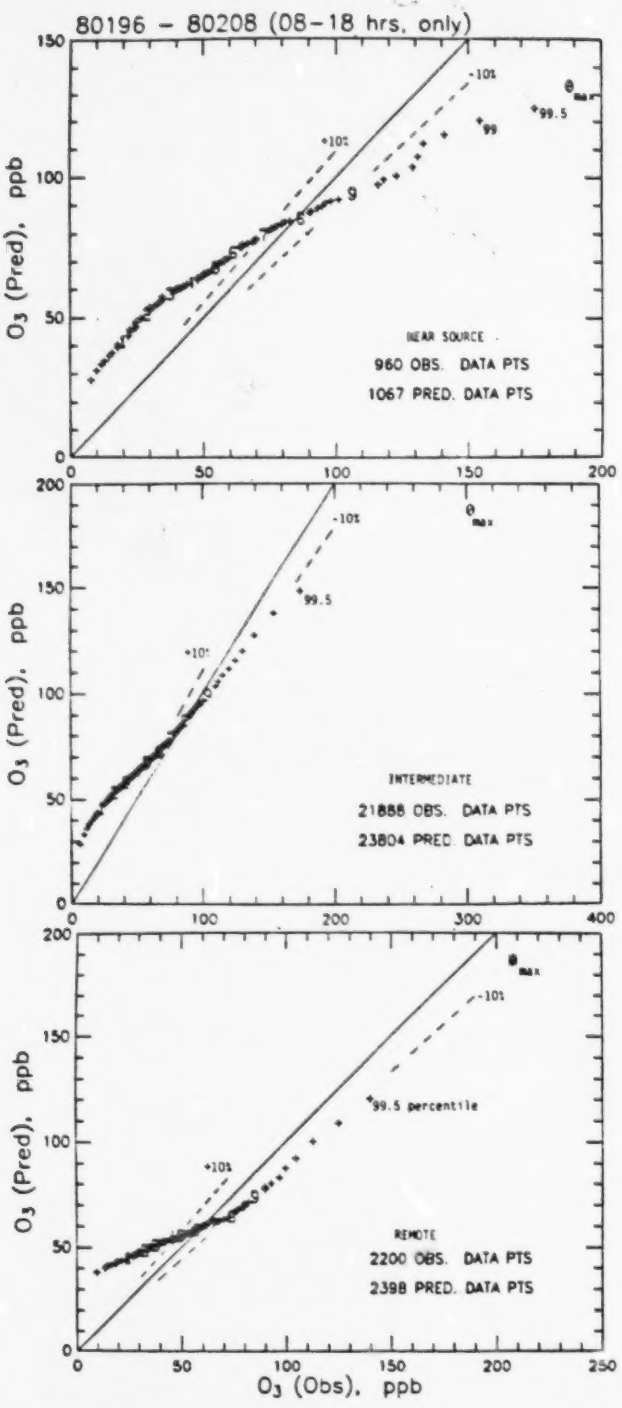

1. Comparison of cumulative frequency distributions of observed (abscissa) and predicted (ordinate) hourly O_3 during the period 14-26 July 1980. Solid lines represent perfect agreement; dashed lines mark ±10% discrepancy bounds. Digits mark decile points, e.g., "0" = 100 percentile or maximum value; "9" = 90-th percentile; etc. The symbol "+" marks integer quantile points except where indicated otherwise. Top panel represents receptor sites in the immediate vicinity of major sources. The middle panel represents receptors between about 5 and 150 km of major sources; and the bottom panel represents receptors farther than about 150 km of major sources.

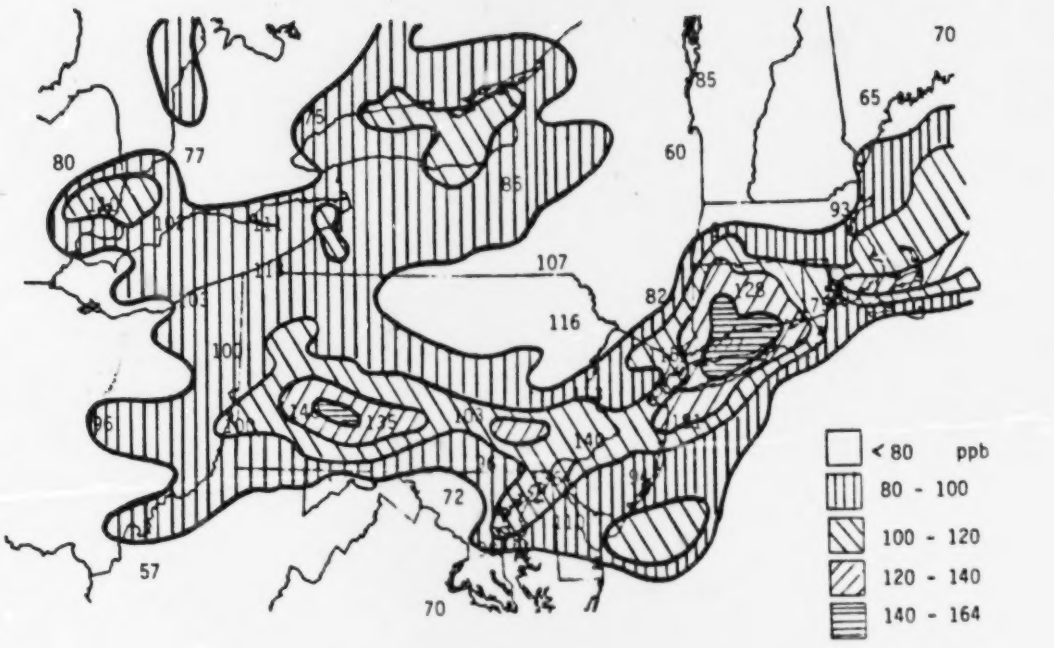

2. Maximum hourly averaged ozone concentration predicted for 20 July 1980 using base level emissions. Numbers are observed values.

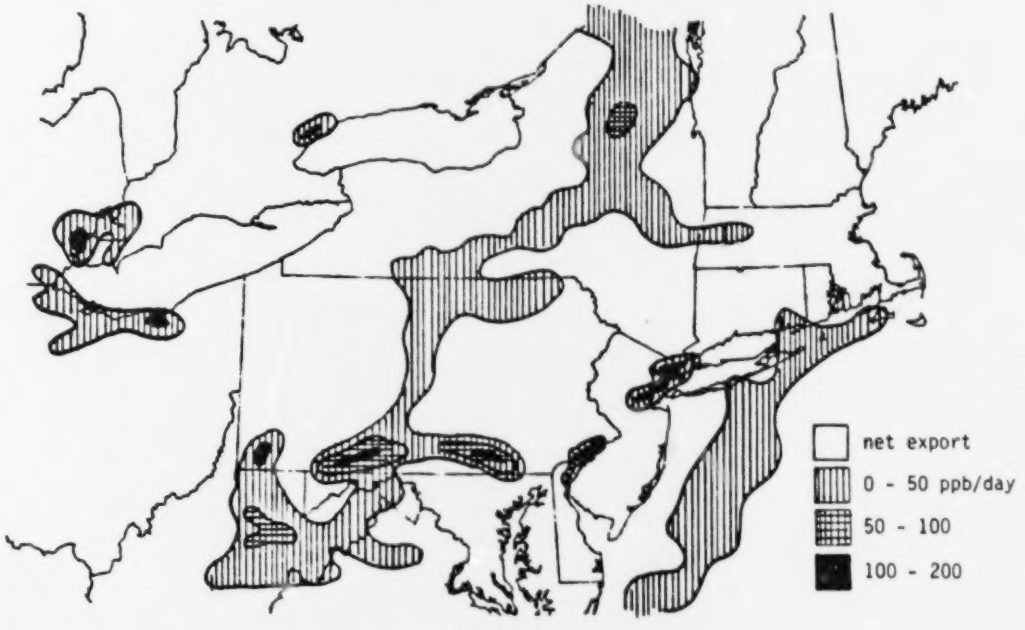

3. Average O_3 transport (horizontal + vertical) for 20 July 1980. Shaded areas had net import of ozone on this day. All other areas were net exporters. Results for Layer 1 only.

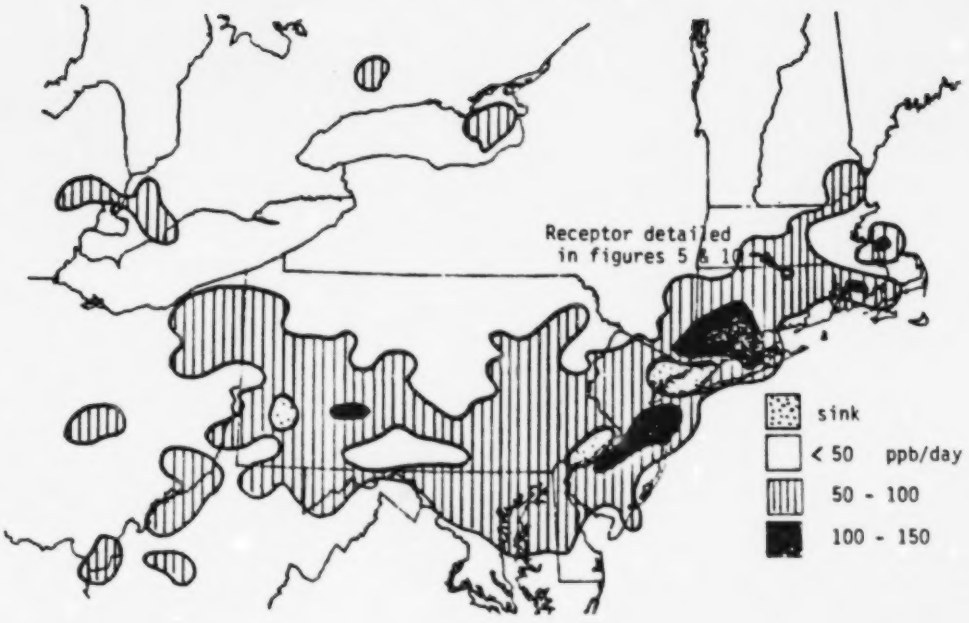

4. Average net production (production - decay) of O_3 for 20 July 1980. Dotted areas are ozone sinks. All other areas are sources. Results for Layer 1 only.

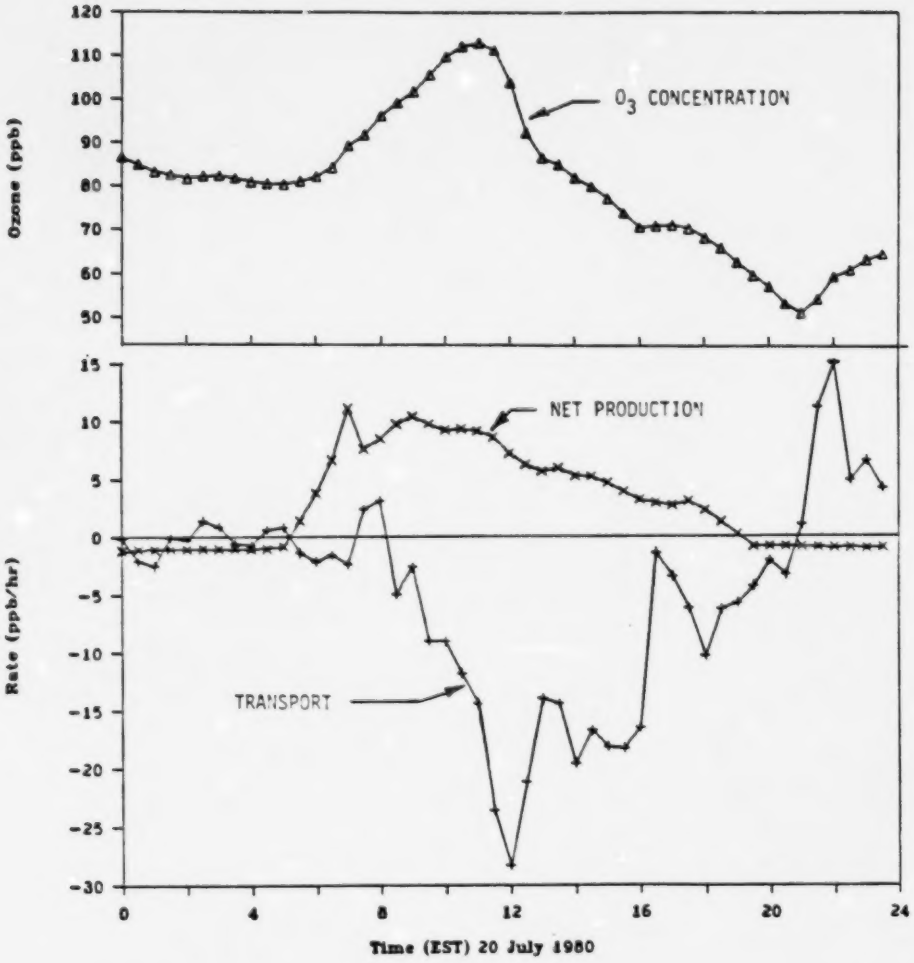

5. Hourly variations of ozone, transport (H+V), and net ozone production (P-D) at the rural Connecticut site marked in Figure 4. Negative transport signifies export of ozone; positive values indicate import. Results for Layer 1 only.

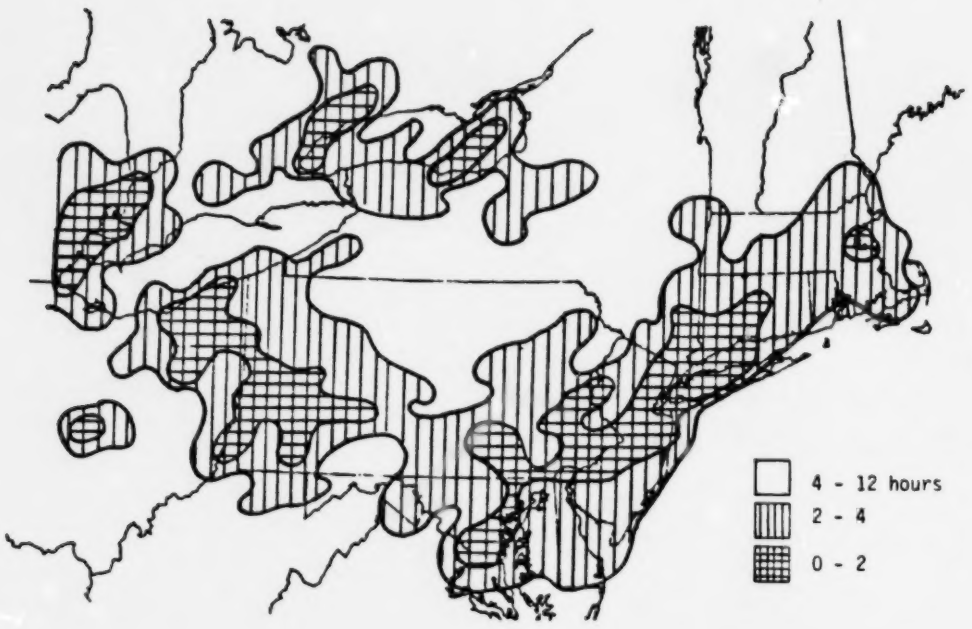

6. Mean lifetime (1/e decay time) of ozone molecules during the daylight hours, 0600-1800 EST, on 20 July 1980. Lifetimes are an order of magnitude larger at night.

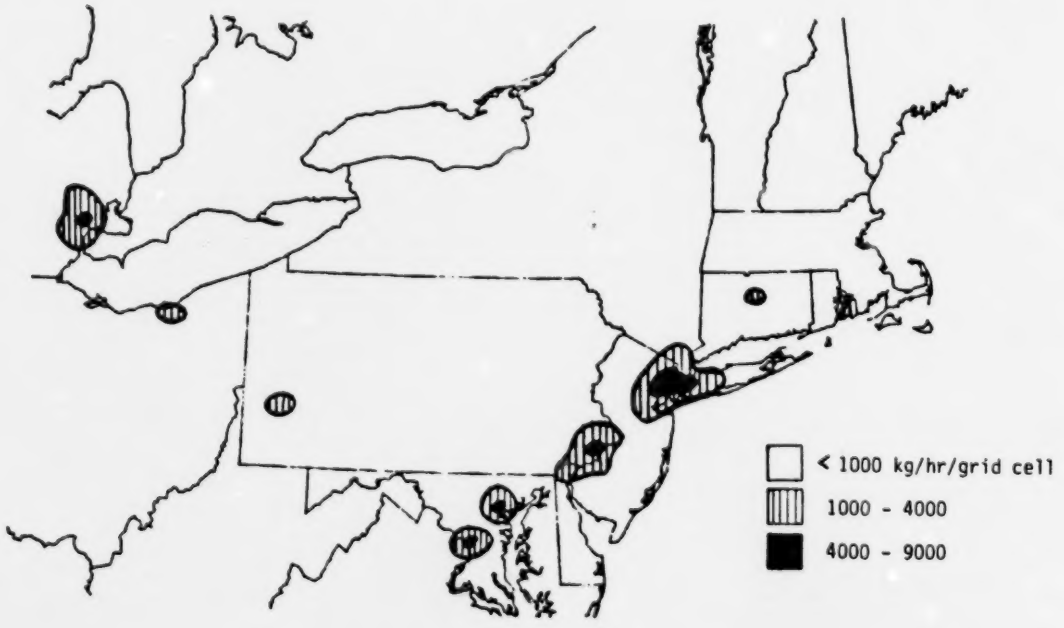

7. Reduction in VOC emissions (kg/hr/grid cell) from the 1980 base levels projected to the 1987 baseline emissions. Only areas with more than 1000 kg/hr/cell reductions are shown. This is referred to in the text as control strategy #1 or CNTRL1. The NO_x and natural hydrocarbon emissions in this strategy are unchanged from the base levels.

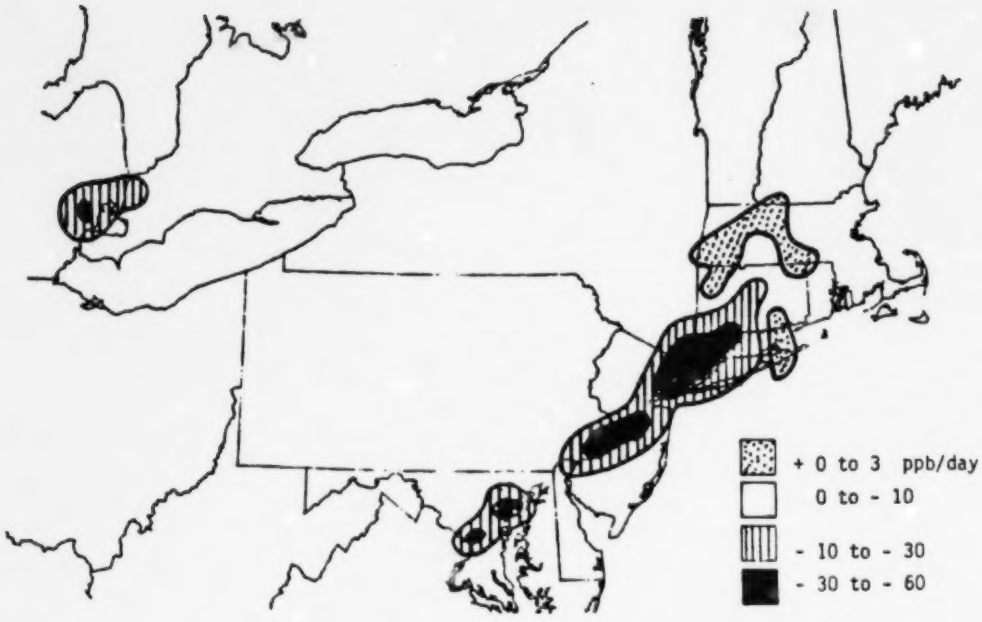

8. Change in the daily net production of ozone on 20 July 1980 effected by control strategy #1 (see Figure 7). Dotted areas mark sites where the ozone production rate is higher with the controlled emissions than with the base, shown in Figure 4. All other areas have reduced production.

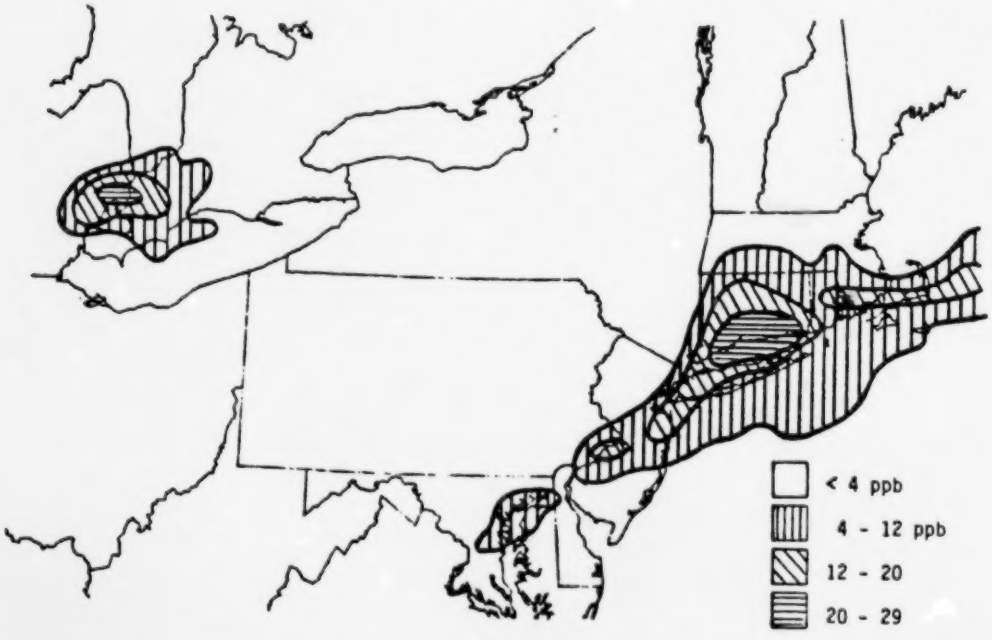

9. Reduction in the daily maximum ozone concentration on 20 July 1980 achieved by control strategy #1 (CNTRL1).

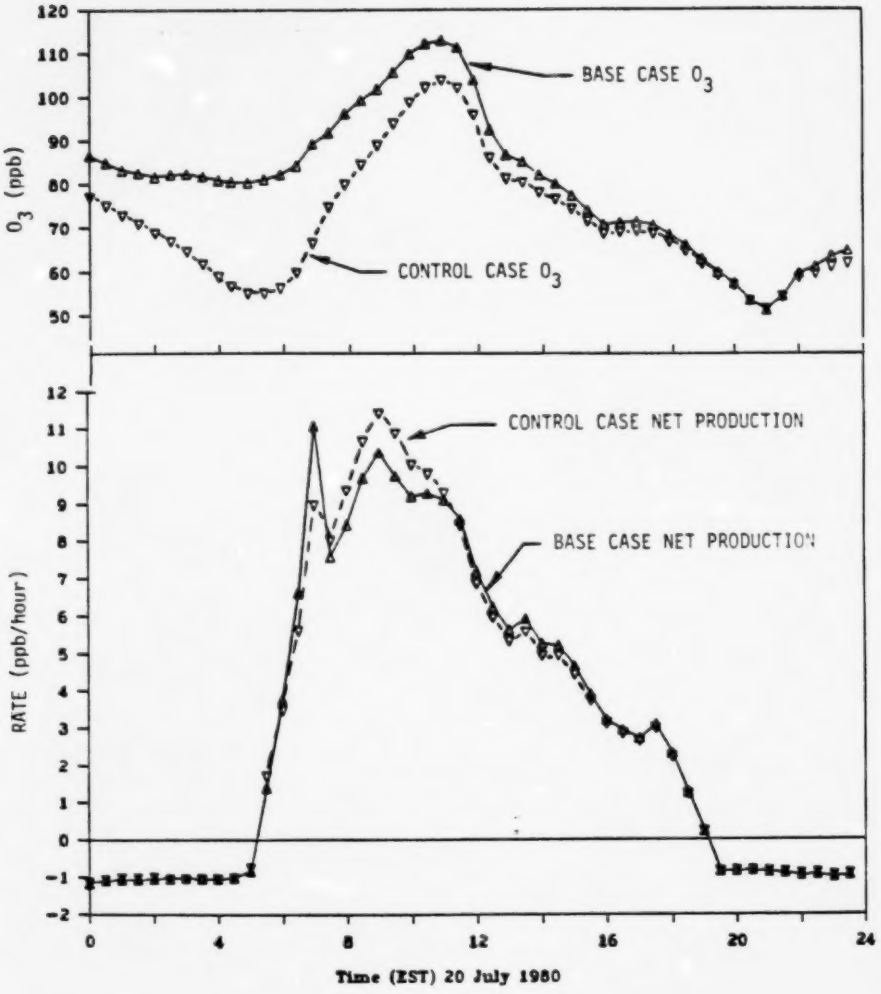

10. Comparison of hourly ozone concentration and net ozone production rate between the base and controlled emissions cases at the rural Connecticut site indicated in Figure 4. The base case concentration and net production profiles shown here are identical to those of Figure 5.

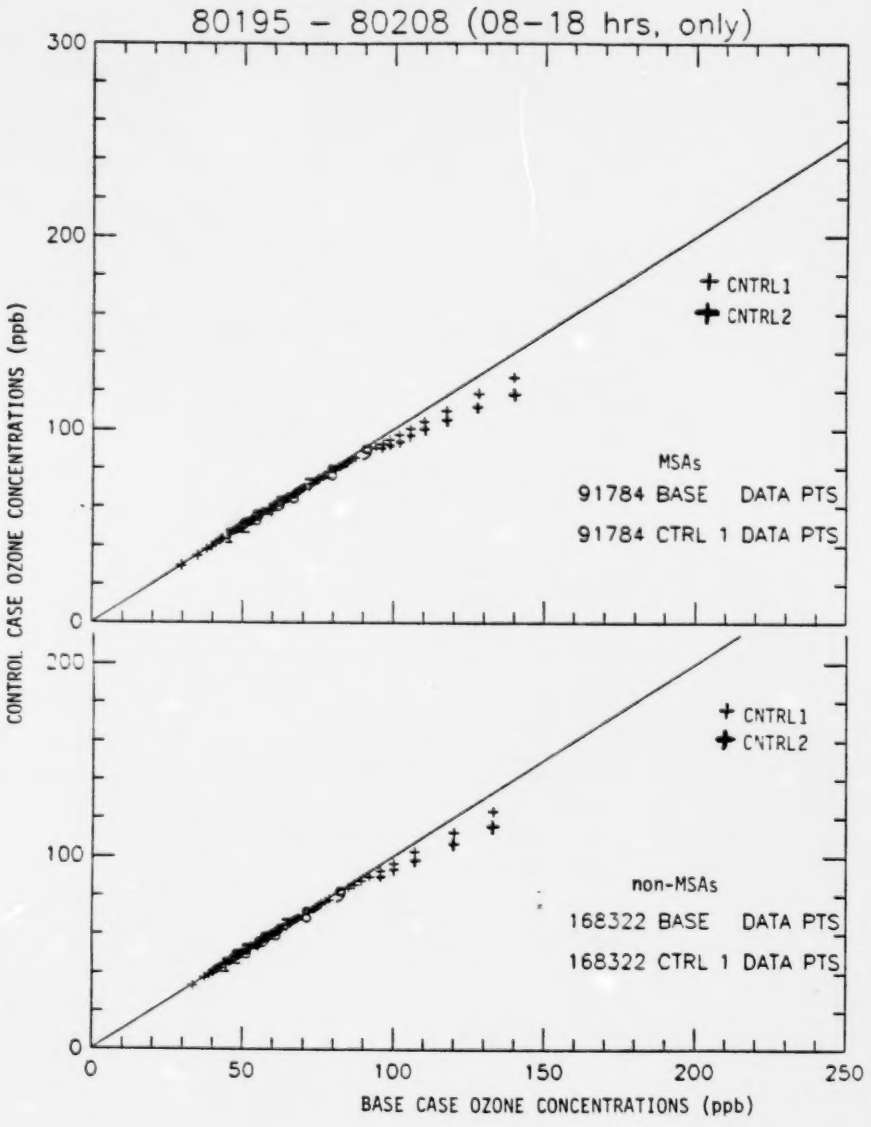

11. Simulated effects of two VOC control strategies on the cumulative frequency distributions of hourly ozone during 13-26 July 1980 at MSA and non-MSA sites. See text for descriptions of the emissions controls in strategies CNTRL1 and CNTRL2.